

Fig. 5 Northern hemisphere view for a 24-hr elliptic orbit.

of Kepler's Second Law is quite visible in this figure. Finally, the motion of a 24-hr elliptic orbit of small eccentricity is shown in Fig. 5. This orbit essentially "rides" up and down the Greenwich meridian as a centerline and always remains on one side of the Earth.

Computer Program Discussion

The original computer program was developed by Baldwin² in the early sixties to display missile trajectories and satellite orbits relative to an Earth background. However, this code was first largely ignored because of its size, complexity, and a few residual "bugs" which caused a certain amount of havoc. Recently, the program's usefulness became apparent during several satellite system design studies and, later, for an actual Earth satellite experiment. Consequently, the existing code was modified and improved and many plots were computed by the author and his colleagues.³⁻⁵

The program is written in Fortran V and is presently running on a Univac 1108 Computer at Lockheed Missiles and Space Co. Depending upon the number of data points forming the orbit, each figure takes from 5 to 15 sec of computer time. In turn, a very large portion of this time is consumed in processing the coastline data and plotting the principal land masses and larger lakes which are visible from the selected viewpoint. For further information, the interested reader is referred to Madigan.⁶

In conclusion, the main purpose of this Note was to present, mostly for the reader's enjoyment, some of the more interesting illustrations which have been obtained during the last few years. A secondary purpose was to announce the existence of such a program to a wide audience.

Table 2 Pertinent plot data

Figure number	Viewpoint L, λ (deg)	Number of points
1	90.0, 0	500
2	60.0, -120.0	400
3	60.0, -120.0	300
4	45.0, -50.0	100
5	45.0, -45.0	100

References

- ¹ "Apollo 16 Brings Us Visions from Space," *National Geographic*, Vol. 142, No. 6, Dec. 1972, pp. 856-865.
- ² Baldwin, H. L., "Orbit Display Using the SC-4020," Rept. 63-0459, 1963, General Dynamics/Astronautics, San Diego, Calif.
- ³ Hitzl, D. L., "Computer Graphics," Internal Note, Oct. 1969, Lockheed Palo Alto Research Lab., Palo Alto, Calif.
- ⁴ Hitzl, D. L. and Shayer, S., "Computer Illustrations," Internal Note, Oct. 1969, Lockheed Palo Alto Research Lab., Palo Alto, Calif.
- ⁵ Hitzl, D. L., "The Relative Motion of Commensurate Earth Satellites," Internal Note, Aug. 1971, Lockheed Palo Alto Research Lab., Palo Alto, Calif.
- ⁶ Madigan, J. T., "Orbit Display Using the SC-4020 Subroutine MPLOTT," Lockheed Missiles and Space Co., Sunnyvale, Calif., 1963.

Mean Flow Development and Surface Heating for an Attaching Compressible Free Shear Layer

DAVID H. RUDY* AND STANLEY F. BIRCH†
NASA Langley Research Center, Hampton, Va.

Introduction

HIGH surface heating rates encountered in regions of shock interference flows are important considerations in design of hypersonic vehicles such as space shuttle. Shock interference patterns have been classified by Edney¹ into six basic types. The present Note considers the interaction resulting when a weak extraneous shock wave impinges on the bow shock of a bluff body inside the sonic line, producing a single shear layer with supersonic flow on one side and subsonic on the other. This interaction, classified as type III by Edney, can occur between the mated booster and orbiter during the ascent phase of a shuttle mission.²

Previous experimental studies of type III interactions have been made by Edney¹ using several geometric shapes as bluff bodies and by Hains and Keyes^{2,3} using a hemisphere. These studies provided surface heating and pressure data for various

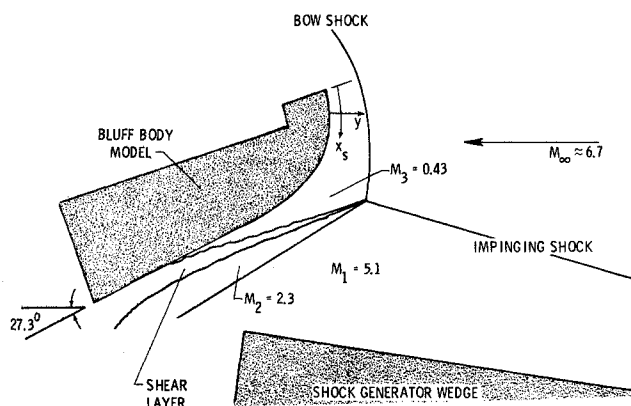


Fig. 1 Flowfield for a typical test condition.

Received September 10, 1973; revision received November 27, 1973.
Index categories: Supersonic and Hypersonic Flow; Jets, Wakes, and Viscid-Inviscid Flow Interactions.

* Aerospace Engineer, Analytical Fluid Mechanics Section, Hypersonic Vehicles Division.

† NASA-NRC Resident Research Associate, Hypersonic Vehicles Division; presently employed at The Boeing Company, Seattle, Wash.

Mach numbers, shear layer impingement angles, and specific heat ratios. Keyes and Morris⁴ presented correlations of the data of Refs. 2 and 3, showing that the surface heat transfer in the attachment region is highly dependent upon whether the shear layer is laminar or turbulent. Birch and Keyes⁵ measured transition Reynolds number for the shear layers in type III interactions. However, none of these studies included detailed surveys of the associated flowfields. The present Note presents shear layer velocity profiles before attachment as well as surface heating and pressure data for a turbulent attaching shear layer in a type III interaction. In the present flow, the shear layer does not stagnate on the model surface since the attachment angle of the shear layer relative to the model surface is small; consequently, reverse flow does not occur in the subsonic region between the shear layer and the surface (unlike the flows in Refs. 1 and 3).

Experimental Results

Mean flow development

The experimental data presented herein were obtained in the Langley 11-in. Hypersonic Tunnel. A sketch of the flowfield is given in Fig. 1 (see Ref. 5 for a schlieren photograph). The nominal freestream Mach number for this facility is 6.8. The actual Mach number varies with total pressure and running time⁶; however, this variation produced no measurable effect on M_2 or M_3 . A 10° wedge was used to generate a planar shock wave which interacted with the bow shock of a bluff body, 7.62 cm (3 in.) long and 6.35 cm (2.5 in.) wide. A stainless steel model instrumented with pressure orifices was used for surface static pressure measurements, and a stycast resin model identical in size and shape to the steel model was used for heat transfer measurements. Velocity profiles were calculated from measured surveys of pitot and static pressure at several flowfield stations before attachment, assuming constant total temperature. These surveys were made with the probes aligned with the flow on the high velocity side.

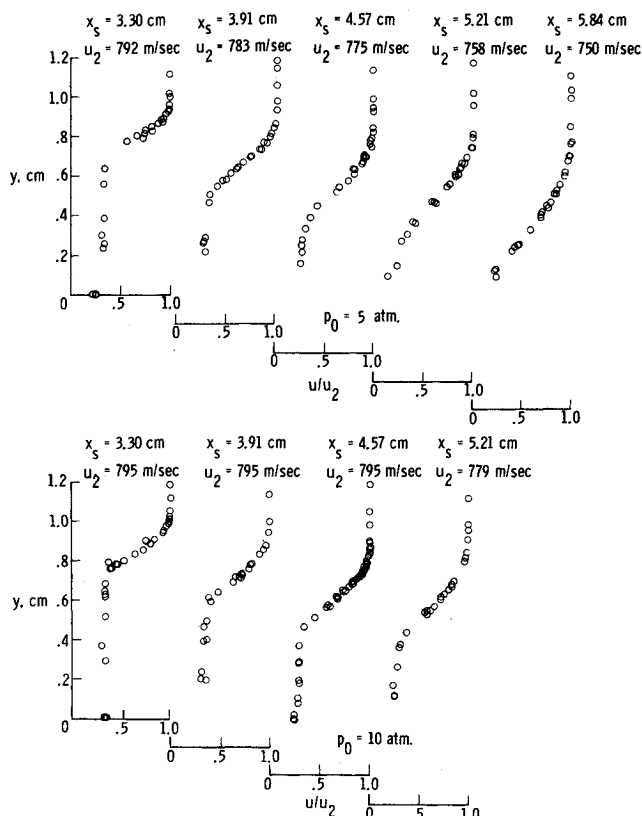


Fig. 2 Centerline mean velocity profiles.

The data were obtained at nominal tunnel stagnation pressures, p_0 , of 5 atm and 10 atm with an average stagnation temperature of 1110R (650°F). The unit Reynolds numbers based on the flow on the high velocity side of the shear layer (region 2) were $3.5 \times 10^5 \text{ m}^{-1}$ ($1.15 \times 10^6 \text{ ft}^{-1}$) and $7.0 \times 10^5 \text{ m}^{-1}$ ($2.3 \times 10^6 \text{ ft}^{-1}$) for total pressures of 5 atm and 10 atm, respectively. Centerline velocity (u/u_2) profiles ahead of the attachment region are presented in Fig. 2 and exhibit the usual "error function" shapes. Plots of constant velocity lines indicate that the shear layers at the two Reynolds numbers are not spreading strictly linearly although at 10 atm an approximately linear spread is observed. The computed spreading parameter, σ (see Birch and Eggers, paper 2 of Ref. 7 for definition), for the 10 atm flow is 30; whereas at 5 atm, the shear layer is spreading approximately 50% faster. If it is assumed that the variation of σ with velocity ratio established for subsonic flows is applicable here, then the measured σ of 30 would correspond to a σ of 16 at a velocity ratio (u_3/u_2) of zero. This is considerably lower than the value obtained for a fully developed Mach 2.3 shear layer as given in paper 2 of Ref. 7. It is, however, close to the expected value if it is assumed that the characteristic Mach number for the flow is the Mach number based on the velocity difference across the shear layer rather than the Mach number on the high velocity side. This indicates that, although the 5 atm shear layer is certainly not spreading at its fully developed rate, the 10 atm shear layer may be approaching it. This interpretation is in agreement with the findings of Morrisette and Birch⁸ who reported that the spreading rate of a shear layer in the near field of a Mach 5 jet increased significantly when the Reynolds number was decreased. They attributed this difference in spreading rate to low Reynolds number effects, indicating that their low Reynolds number flow was not fully developed. Low Reynolds number effects are also discussed by Birch and Eggers (paper 2 of Ref. 7). While the present results suggest a similar conclusion, the result is less definitive here because of the close proximity of the shear layer to the model surface. Surface static pressure measurements on the bluff body show a symmetric drop in static pressure of $1.03 \times 10^4 \text{ n/m}^2$ (0.15 psia) and $1.72 \times 10^4 \text{ n/m}^2$ (0.25 psia), respectively, for 5 atm and 10 atm between the centerline and near the model edge. Although this static pressure gradient indicates some crossflow, its low level suggests that the three-dimensional effects are probably confined to the low velocity side of the shear layer close to the bluff body. It should also be noted that while the shear stress levels in a radial free-jet¹⁰ and a radial wall jet¹¹ are approximately twice as large as the levels in the corresponding two-dimensional flows, there is little change in the over-all spreading rate. There is, therefore, no a priori reason for believing that a small crossflow would substantially alter the spreading rates in the present shear layers if the present flows were fully developed.

In the present experiments, the initial thickness of the shear layer is very small (same order of magnitude as the shock thickness). The apparent persistence of low Reynolds number effects up to 10 atm suggests that the appropriate criterion for fully developed flow is a Reynolds number criterion rather than a criterion simply based on the number of initial boundary-layer thicknesses. This interpretation is in agreement with the results found by Bradshaw⁹ for subsonic shear layers. However, as Bradshaw notes (pp. 39–40, Ref. 7) the physical basis for this conclusion is not obvious; therefore, the results should be used with some caution, particularly for flows which differ significantly from those reported here.

Surface heating and pressure

Heat-transfer data were obtained at the same tunnel conditions previously described using the phase-change coating technique.¹² The 11-in. Tunnel was not equipped with an injection system; therefore, the model was exposed to the flow during the short time the tunnel total temperature and total pressure were rising to steady-state values. Only data taken at times at least twice the length of the tunnel total temperature transient were used, since calculations showed that such data were relatively un-

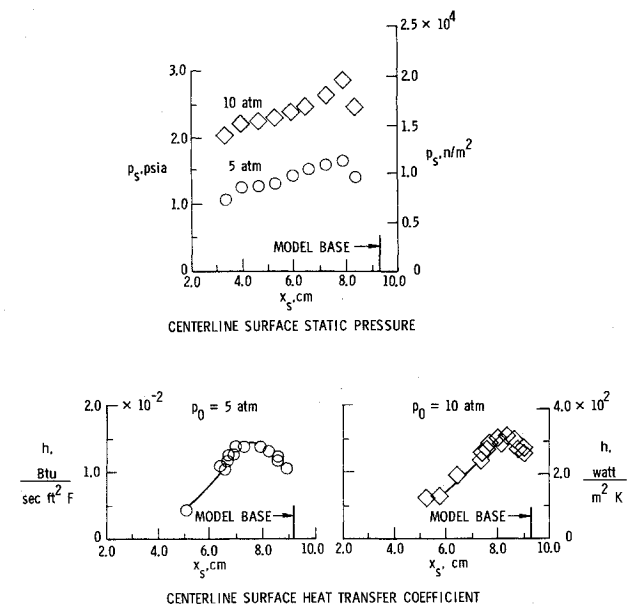


Fig. 3 Surface static pressure and heating in attachment region.

affected by the short transient. (The surface heat-transfer coefficient, h , varied less than 5% from the value for constant total temperature for long melt times.) In addition, the data reduction method of Hunt et al.,¹³ which incorporates into the solution the measured total temperature variation, was used. The over-all error associated with the data reduction procedure is estimated to be no more than 10–15%.

The surface centerline heat-transfer data in the attachment region are shown in Fig. 3 along with the centerline surface static pressure. The static pressure increases with x_s , dropping off at the last pressure measurement station because of its nearness to the base of the model. Since the heating data for each total pressure represent measurements from several runs, the scatter in the data is attributed to slight variations in test conditions between these runs. The peak value of h is 6% higher at 10 atm than at 5, with the peak occurring at an x_s of 0.635 cm (0.25 in.) further back on the model surface at 10 atm. This difference is partially caused by a change in location of the shock interaction produced by a difference in boundary-layer displacement thickness on the shock generator wedge at the

lower unit Reynolds number. This changes slightly the angle of the impinging shock wave and, hence, the interaction location.

These data are compared with the turbulent data of Ref. 3 in Fig. 4 where measured peak Stanton number, $h_{\text{peak}}/(\rho_w u_4 C_p)$, is plotted as a function of Reynolds number based on shear layer thickness at attachment (δ_{SL}), $(\rho_w u_4 \delta_{SL})/(\mu_w \sin \theta_{SL})$. The density, ρ_w , and the viscosity, μ_w , are based on measured surface temperature and measured peak static pressure. θ_{SL} is the shear layer angle relative to model surface inclination. u_4 is the velocity in the region behind the oblique shock that usually occurs at the attachment point (see Fig. 5 of Ref. 3). In the present study the attachment occurred near the base of the model and no oblique shock occurred. Therefore, an approximation to u_4 was computed using u_2 assuming an oblique shock at the attachment point and flow parallel to an extended model surface behind the shock. The Keyes-Hains data and correlation represent shear layers which are three dimensional in nature with relatively large (27°–42°) attachment angles. Also shown is the correlation of Bushnell and Weinstein¹⁴ for reattaching two-dimensional turbulent boundary layers which, in general, represents data at relatively low attachment angles. The present data with an intermediate range value of θ_{SL} (18.6°) and some three-dimensional effects fall between these two correlations. In addition, the 10 atm data point falls closer to the Bushnell-Weinstein correlation, indicating perhaps that this flow is less influenced by three-dimensional effects than the 5 atm flow.

Summary

Mean velocity profiles in the $M_2 = 2.3$ attaching free shear layer of a type III shock interaction were experimentally measured. The spreading rate indicates that the turbulent shear layer flow was not fully developed. Surface heating and static pressure were also measured and the peak heating was compared with available two- and three-dimensional attaching shear layer data. The present 10 atm data were found to be less influenced by three-dimensional effects than the 5 atm data.

References

- 1 Edney, B., "Anomalous Heat Transfer and Pressure Distributions on Blunt Bodies at Hypersonic Speeds in the Presence of an Impinging Shock," FFA Rept. 115, 1968, The Aeronautical Research Institute of Sweden, Stockholm, Sweden.
- 2 Hains, F. D. and Keyes, J. W., "Shock Interference Heating in Hypersonic Flows," *AIAA Journal*, Vol. 10, No. 11, Nov. 1972, pp. 1441–1447.
- 3 Keyes, J. W. and Hains, F. D., "Analytical and Experimental Studies of Shock Interference Heating in Hypersonic Flows," TN D-7139, May 1973, NASA.
- 4 Keyes, J. W. and Morris, D. J., "Calculations of Peak Heating in Shock Interference Regions at Hypersonic Speeds," *Journal of Spacecraft and Rockets*, Vol. 9, No. 8, Aug. 1972, pp. 621–623.
- 5 Birch, S. F. and Keyes, J. W., "Transition in Compressible Free Shear Layers," *Journal of Spacecraft and Rockets*, Vol. 9, No. 8, Aug. 1972, pp. 623–624.
- 6 McLellan, C. H., Williams, T. W., and Beckwith, I. E., "Investigation of the Flow Through a Single-Stage Two-Dimensional Nozzle in the Langley 11-inch Hypersonic Tunnel," TN 2223, Dec. 1950, NACA.
- 7 *Free Turbulent Shear Flows. Vol. I—Conference Proceedings*, NASA SP-321, 1973.
- 8 Morrisette, E. L. and Birch, S. F., "Mean Flow and Turbulence Measurements in a Mach 5 Shear Layer, Part I—The Development and Spreading of the Mean Flow," *Fluid Mechanics of Mixing*, American Society of Mechanical Engineers, New York, 1973, pp. 79–82.
- 9 Bradshaw, P., "The Effect of Initial Conditions on the Development of a Free Shear Layer," *Journal of Fluid Mechanics*, Vol. 26, Pt. 2, 1966, pp. 225–236.
- 10 Heskestad, G., "Hot-Wire Measurements in a Radial Turbulent Jet," *Journal of Applied Mechanics*, Vol. 33, Ser. G, No. 2, June 1966, pp. 417–424.
- 11 Bradshaw, P., "Variations on a Theme of Prandtl," *Turbulent Shear Flows*, AGARD-CP-93, Sept. 1971, C-1–C-10.
- 12 Jones, R. A. and Hunt, J. L., "Use of Fusible Temperature Indicators for Obtaining Quantitative Aerodynamic Heat-Transfer Data," TR R-230, Feb. 1966, NASA.

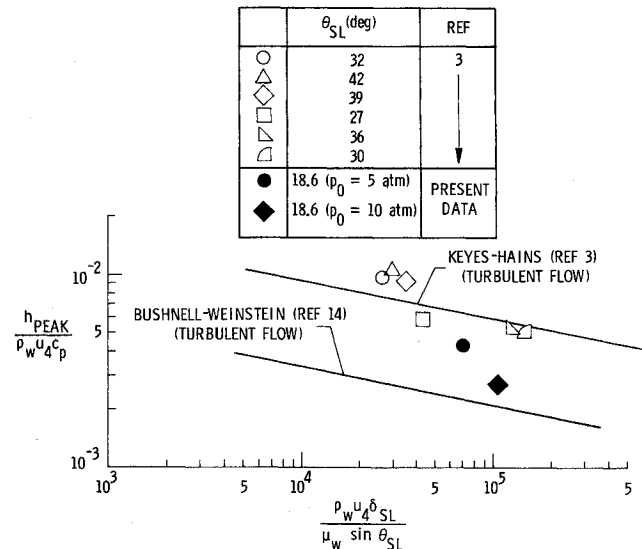


Fig. 4 Comparison of peak heat-transfer data with other data.

¹³ Hunt, J. L., Pitts, J. I., and Richie, C. B., "Application of Phase-Change Technique to Thin Sections with Heating on Both Surfaces," TN D-7193, 1973, NASA.

¹⁴ Bushnell, D. M. and Weinstein, L. M., "Correlation of Peak Heating for Reattachment of Separated Flows," *Journal of Spacecraft and Rockets*, Vol. 5, No. 9, Sept. 1968, pp. 1111-1112.

Subscripts

eq = equilibrium

j = slot

t = total or stagnation

∞ = freestream

Swept-Slot Film-Cooling Effectiveness in Hypersonic Turbulent Flow

JERRY N. HEFNER* AND AUBREY M. CARY Jr.†
NASA Langley Research Center, Hampton, Va.

Nomenclature

- M = Mach number
 s = slot height
 T = temperature
 u = velocity
 x = coordinate in freestream direction
 y = coordinate normal to plate surface
 ϵ = effectiveness parameter $(T_{t,\infty} - T_{eq})/(T_{t,\infty} - T_{t,j})$
 λ = mass flow parameter, $\rho_j u_j / \rho_\infty u_\infty$
 ρ = density
 Λ = slot sweep angle in plane of the flat plate
 θ = surface streamline direction relative to x -axis

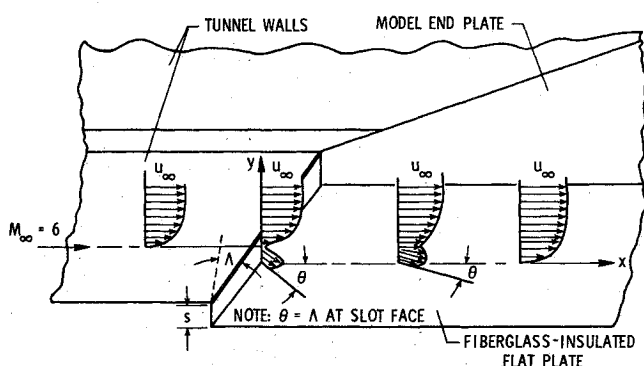


Fig. 1 Swept-slot film-cooling model.

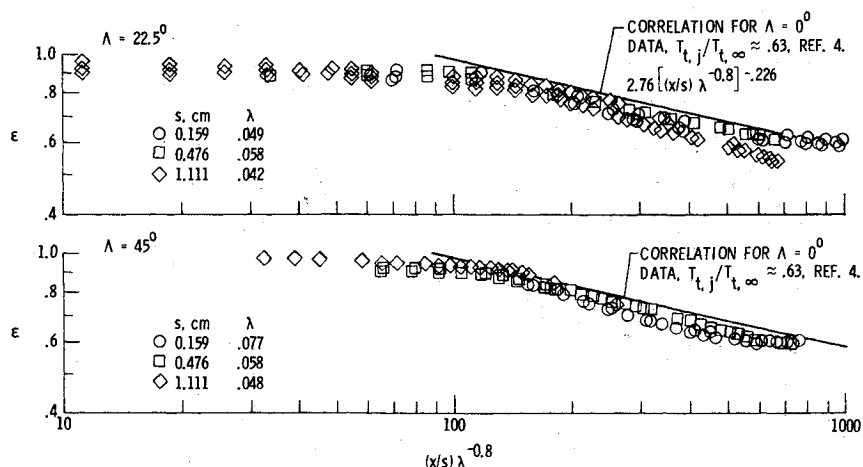
Introduction

FILM cooling provides a means of reducing the operational surface temperature of a high-speed vehicle below the radiation equilibrium temperature. Experimental studies of tangential slot injection at Mach 6^{1,2} have shown that the film-cooling effectiveness in a two-dimensional, high-speed turbulent flow is significantly greater than indicated by extrapolations of previous low-speed results. However, practical applications of slot injection film cooling (particularly on wings) will generally require the slots to be swept relative to the inviscid streamline direction. The effect of sweeping the slot on the film-cooling effectiveness downstream of the slot has not been previously investigated. The present Note presents measurements of surface equilibrium temperature downstream of swept slots with sonic tangential air injection into a thick hypersonic turbulent boundary layer and compares these results with unswept slot results.³

Experimental Approach

The experimental investigation was conducted in the Langley 20-in. Mach 6 wind tunnel⁴ at a freestream total temperature and unit Reynolds number per centimeter of 492°K and 0.287×10^6 , respectively. The model (see Fig. 1) was a fiberglass flat plate (35.5 cm wide and 91.4 cm long) mounted parallel with and recessed below the flat tunnel wall. The slot flow was ejected tangentially over the surface of the flat plate from a two-dimensional sonic slot swept at either 22.5° or 45° relative to the freestream flow. The slot flow was ejected normal to the slot and was swept at either 22.5° or 45° relative to the freestream direction. The slot configuration could be adjusted to provide slot heights of 0.159, 0.476, and 1.111 cm with the outer slot wall thickness (wall between slot flow and freestream) held constant at 0.159 cm. The slot flow temperature was varied from 136°K to 311°K. The slot mass flow rate was uniform over a midspan of at least 21 cm and could be metered to insure sonic slot injection. Surface temperatures were measured by flush-mounted thermocouples located along the centerline of the insulated flat plate surface. The surface temperatures were considered to be in equilibrium when for a period of at least 100 sec they changed less than 0.1%.

Fig. 2 Film-cooling effectiveness for $T_{t,j}/T_{t,\infty} \approx 0.60$.



Received November 13, 1973; revision received January 22, 1974.

Index categories: Boundary Layers and Convective Heat Transfer—Turbulent; Supersonic and Hypersonic Flow.

* Aerospace Engineer, Analytical Fluid Mechanics Section, Hypersonic Vehicles Division. Member AIAA.

† Head, Applied Fluid Mechanics Section, Hypersonic Vehicles Division. Member AIAA.